International Journal of Infectious Diseases 122 (2022) 1009–1017

Contents lists available at ScienceDirect

International Journal of Infectious Diseases

journal homepage: www.elsevier.com/locate/ijid

# Understanding the transmission dynamics of a large-scale measles outbreak in Southern Vietnam

Thi Huyen Trang Nguyen[1,2,*], Thuong Vu Nguyen[2], Quang Chan Luong[2], Thang Vinh Ho[2], Christel Faes[1], Niel Hens[1,3]

[1] Hasselt University, 3500 Hasselt, Belgium
[2] The Pasteur Institute in Ho Chi Minh City, 70000 Ho Chi Minh City, Vietnam
[3] The University of Antwerp, 2000 Antwerp, Belgium

ARTICLE INFO

*Article history:*
Received 17 January 2022
Revised 21 July 2022
Accepted 21 July 2022

*Keywords:*
Spatio-temporal analysis
Vaccine preventable disease
Measles
Vietnam

ABSTRACT

*Objectives:* Southern Vietnam experienced a large measles outbreak of over 26,000 cases during 2018-2020. We aimed to understand and quantify the measles spread in space-time dependence and the transmissibility during the outbreak.

*Methods:* Measles surveillance reported cases between January 2018 and June 2020, vaccination coverage, and population data at provinicial level were used. To illustrate the spatio-temporal pattern of disease spread, we employed the endemic-epidemic multivariate time series model decomposing measles risk additively into autoregressive, spatio-temporal, and endemic components. Likelihood-based estimation procedures were performed to determine the time-varying reproductive number $R_e$ of measles.

*Results:* Our analysis showed that the incidence of measles was associated with vaccination coverage heterogeneity and spatial interaction between provincial units. The risk of infections was dominated by between-province transmission (36.1% to 78.8%), followed by local endogenous transmission (4.1% to 61.5%). In contrast, the endemic behavior had a relatively small contribution (2.4% to 33.4%) across provinces. In the exponential phase of the epidemic, $R_e$ was above the threshold with a maximum value of 2.34 (95% CI: 2.20-2.46).

*Conclusion:* Local vaccination coverage and human mobility are important factors contributing to the measles dynamics in Southern Vietnam, and the high risk of inter-provincial transmission is of most concern. Strengthening the disease surveillance is recommended, and further research is essential to understand the relative contribution of population immunity and control measures in measles epidemics.



## Introduction

Measles is an infectious disease transmitted via the respiratory route. Despite remarkable progress in reducing global disease incidence especially from 2000 to 2016, the incidence increased again in 2019 and major outbreaks occurred in a number of countries (Andrianou *et al.*, 2019; Nimpa *et al.*, 2020; Patel *et al.*, 2020; Pogka *et al.*, 2020; Zucker *et al.*, 2020). Many studies indicated the spatio-temporal variability of measles incidence and transmission is because of the discrepancy in vaccination coverage between geographical units (Herzog *et al.*, 2011; Robert *et al.*, 2022) and human movement (Parpia *et al.*, 2020; Qin *et al.*, 2019), which plays an important role in the spatial spreading of the virus. Furthermore, unobserved heterogeneity such as underreporting may affect the heterogeneity of incidence levels (Paul and Held, 2011). Understanding these characteristics and their impacts on transmission dynamics of measles outbreaks is therefore crucial for effectively tailoring control strategies, including immunization and surveillance activities.

Between 2018 and 2020, Vietnam experienced the largest measles outbreak in the last two decades. The Southern region was the worst affected area, where the incidence in 2019 exceeded by sevenfold the government's annual indicator of 7.5 cases per 100,000 population (Vietnam Ministry of Health, 2020). In this region, measles cases were disproportionately distributed, and incidence was greatly heterogeneous across cities and provinces (hereinafter referred to as provinces). In this study, we aimed to quantify the spatio-temporal variability of the transmission of measles

* Corresponding author: Thi Huyen Trang Nguyen, Data Science Institute, Hasselt University, 3500 Hasselt, Belgium, Tel: +32477381286.
*E-mail address:* thihuyentrang.nguyen@uhasselt.be (T.H.T. Nguyen).

https://doi.org/10.1016/j.ijid.2022.07.055

in this outbreak by performing an analysis of the time series of measles cases in Southern Vietnam from January 1, 2018, to June 30, 2020. We used the endemic-epidemic statistical modeling framework (Held *et al.*, 2005; Paul *et al.*, 2008), which decomposes the risk of infections additively into autoregressive, spatio-temporal, and endemic components. Accordingly, the occasional outbreaks are determined by autoregression on past counts of within- and between localities, whereas the disease background is described by the endemic component that is explained by exogenous factors independent of the epidemic. We also estimated the time-varying reproduction number $R_e(t)$ to understand the disease transmission intensity of the outbreak using the procedure by Wallinga and Teunis (2004). Routine surveillance data of measles daily counts stratified by provincial level and other additional data sources such as the population data and the vaccination coverage data of measles-containing vaccine (MCV) were included in the analysis.

## Methods

### *Data sources*

#### *Routine surveillance data*

Our study focused on two cities and 18 provinces of Southern Vietnam, including the province of Lam Dong and 19 provincial units in the Mekong River Delta and South East areas. On October 11, 2020, we extracted 26,047 individual measles cases reported between January 1, 2018, to June 30, 2020, in the study setting from the Electronic Communicable Disease Surveillance system (https://baocaobtn.vncdc.gov.vn/). To analyze spatio-temporal spread of the disease, we aggregated the number of cases by date of onset and by province. Data cleaning and descriptive analysis were carried out using the Microsoft Excel and R software version 4.0.2.

#### *Vaccination coverage data*

The yearly vaccination coverage data of the first doses of MCV (MCV1) reported in 2019 were sourced from the Expanded Program on Immunization (EPI) Unit at the Pasteur Institute in Ho Chi Minh City for modeling purposes. The MCV1 coverage was stratified by province, ranging from 82.7% in Binh Phuoc to 99.8% in Lam Dong. This coverage was taken fixed through time.

#### *Population data*

We adopted the province-specific demographic data from the 2019 Vietnam Population and Housing Census (General Statistics Office of Vietnam, 2020). The total population comprised 36,399,443 people in 2019 and was assumed to be constant over 2018-2020.

### *Estimation of* $R_e$

We estimated $R_e$ at time $t$ following the approach by Wallinga and Teunis (2004), which is a likelihood-based estimation procedure based on reported cases, and assuming fixed serial interval distribution (i.e., the time between onset days of two paired cases). We assumed that the serial interval of measles is normally distributed with a mean of 11.9 days and a standard deviation of 2.6 days (Vink *et al.*, 2014). $R_e$ and the 95% confidence intervals (95% CIs) were estimated using the EpiEstim package (Cori *et al.*, 2013). To increase the precision of the estimated $R_e$, we ran 100 simulations and used 21-day time windows corresponding to the definition of outbreak termination in the National Surveillance Guideline (Vietnam Ministry of Health, 2012). An outbreak of measles is declared terminated if no new cases are identified within 21 days after the symptom onset of the last laboratory-confirmed or epidemiologically linked case.

### *The endemic-epidemic multivariate time series model*

The model we employed was introduced by Held *et al.* (2005) and assumes that conditionally on past counts, the number of cases reported in province $r$ ($r = 1, \ldots, R$) at time $t = 1, \ldots, T$, denoted as $Y_{rt}$, follows a negative binomial distribution with mean $\mu_{rt}$ and a conditional variance $\mu_{rt}(1 + \mu_{rt}\psi)$ with overdispersion parameter $\psi > 0$. Note that when $\psi \equiv 0$, it simplifies to the Poisson distribution. Generally, the mean $\mu_{rt}$ is decomposed into an endemic component, which serves as baseline number of cases, and an observation-driven epidemic component, which represents the impact of number of past cases at time $t-1$ in the same (i.e., autoregressive effects) or other regions (i.e., neighborhood effects):

$$\mu_{rt} = e_{rt}\nu_{rt} + \lambda_{rt}Y_{r,t-1} + \phi_{rt}\sum_{r' \neq r} w_{r'rimer}Y_{r'rime,t-1} \quad \text{(i)}$$

with transmission weights $w_{r'r}$, for which $w_{rr} = 0$. The non-negative factors $\nu_{rt}$, $\lambda_{rt}, \phi_{rt}$ are modeled on a log scale:

$$\log(\nu_t) = \alpha^{(\nu)} + b_r^{(\nu)} + \beta_t t + \gamma \sin(\omega t) + \delta \cos(\omega t) + \alpha_{vac}\log(1 - \upsilon_r), \quad \text{(ii)}$$

$$\log(\lambda_{rt}) = \alpha^{(\lambda)} + b_r^{(\lambda)} + \beta_{vac}\log(1 - \upsilon_r), \quad \text{(iii)}$$

$$\log(\phi_{rt}) = \alpha^{(\phi)} + b_r^{(\phi)} + \tau\log(e_{rt}). \quad \text{(iv)}$$

The three equations above contain component-specific fixed intercepts ($\alpha^{(\nu)}$, $\alpha^{(\lambda)}$, $\alpha^{(\phi)}$), random effects ($b_r^{(\nu)}, b_r^{(\lambda)}, b_r^{(\phi)}$), and regression terms, which allow for seasonal varying incidence (Held and Paul, 2012; Paul *et al.*, 2008; Paul and Held, 2011), but may also include exogenous covariate vectors such as vaccination coverage (Herzog *et al.*, 2011) and population size (Xia *et al.*, 2004). First, assuming that the epidemic incorporates cases within a province and from adjacent provinces only (i.e., first-order neighbors, $w_{r'r} = 1$), the basic model formulation follows the equation (i) where the endemic component is assumed to vary seasonally with a trend parameter $\beta_t$, a sine-cosine term with amplitude $A = \sqrt{\gamma^2 + \delta^2}$, a phase shift $\varphi$ ($\tan(\varphi) = \delta/\gamma$), and the sinusoidal wave of frequency $\omega$ identified as $2\pi/365$ for daily continuous measurements and is modeled proportional to the population $e_{rt}$ (Held and Paul, 2012), the two epidemic components only contain intercepts. Second, as an extension to this model, the vaccination coverage of MCV1, $\upsilon_r$, is included in the model as a covariate (Herzog *et al.*, 2011). Specifically, the province-specific proportion of unvaccinated population, $1 - \upsilon_r$, used as a proxy for susceptibility of the population to measles, was log-transformed in the endemic and autoregressive components with coefficients $\alpha_{vac}$ and $\beta_{vac}$, respectively. Next, the inclusion of the log-population effects in the spatio-temporal component (i.e., neighborhood effects) is worth considering in our study, as it has proven useful reflecting the agglomeration effects, in which the power of the population scaling factor $\tau$ is to be estimated (Meyer and Held, 2014; Xia *et al.*, 2004). Furthermore, the importance of higher-order neighboring provinces in disease transmission can be assessed using the power law model, which allows for measuring of the transmission weights $w_{r'r} = o_{r'r}^{-d}$, where the decay parameter $d > 0$ is to be estimated (Meyer and Held, 2014) and $o_{r'r}$ is the adjacency order. We considered that two distinct units $r'$ and $r$ are $k$th-order neighbors (i.e., $o_{r'r} = o_{rr'} = k$) if the shortest distance between them has $k$ steps across geographical units. In our setting, $k$ ranges from 1 to 7. Finally, to address the unobserved heterogeneity of disease transmission such as underreporting and "edge effects" (i.e., cases can be sourced from areas outside of the study setting), we introduced independent random effects $b_r^{(\nu)}, b_r^{(\lambda)}, b_r^{(\phi)}$ in the three components of the model (Paul and Held, 2011). The influence of

**Table 1**
Glossary of notation for spatio-temporal model parameters.

| Notation | Parameter |
|---|---|
| $\ell$ | Log-likelihood |
| $\ell_{pen}$ | Penalized log-likelihood |
| $\ell_{marg}$ | Marginal log-likelihood |
| *maxEV* | Maximum eigenvalue |
| AIC | Akaike information criterion |
| $\alpha^{(\lambda)}$ | Fixed effect, autoregressive component |
| $\alpha^{(\phi)}$ | Fixed effect, spatio-temporal component (neighborhood effects) |
| $\alpha^{(\nu)}$ | Fixed effect, endemic component |
| $b_r^{(\lambda)}$ | Random effects, autoregressive component |
| $b_r^{(\phi)}$ | Random effects, spatio-temporal component (neighborhood effects) |
| $b_r^{(\nu)}$ | Random effects, endemic component |
| $\sigma^2_\lambda$ | Variance, autoregressive random effects |
| $\sigma^2_\phi$ | Variance, spatio-temporal random effects |
| $\sigma^2_\nu$ | Variance, endemic random effects |
| $d$ | Distance decay |
| $\tau$ | The power of the population scaling factor |
| $\alpha_{vac}$ | Covariate (vaccination coverage) coefficient in endemic component |
| $\beta_{vac}$ | Covariate (vaccination coverage) coefficient in autoregressive component |
| $\psi$ | Overdispersion |
| $\beta_t$ | Trend parameter |
| $\omega$ | The sinusoidal wave of frequency identified as $2\pi/365$ |
| $A$ | Amplitude of seasonal variation, $A = \sqrt{\gamma^2 + \delta^2}$ |
| $\varphi$ | Phase shift $\varphi$, with $\tan(\varphi) = \delta/\gamma$ |

the epidemic component on the overall disease incidence is investigated by the dominant eigenvalue (*maxEV*). If the eigenvalue is $< 1$, it can be interpreted as the proportion of epidemic potential of disease incidence, otherwise it expresses an outbreak period (Meyer and Held, 2014; Held and Paul, 2012). We assumed that the mixing behavior is homogeneous. Our multivariate time series models were fitted via (penalized) maximum likelihood. All the notations are listed in Table 1.

The performance of models was based on the comparison of one-step-ahead predictions based on the observed data by using proper scoring rules (Czado *et al.*, 2009; Paul and Held, 2011). Lower scores correspond to better prediction. In our study, we utilized the logarithmic score (logS) and ranked probability score (RPS) regarding both sharpness, the concentration of the predictive distributions, and calibration, the statistical consistency between the probabilistic forecasts and the observation (Czado *et al.*, 2009). The difference between scores from two models was tested by the permutation test (Czado *et al.*, 2009; Paul and Held, 2011).

All procedures were performed using the R package surveillance version 1.19.1, "hhh4" class (Meyer *et al.*, 2017).

See Supplementary for more details on the used models.

## Results

### *Descriptive analysis*

A total of 26,047 measles cases (55.4% male) and one measles-attributable death were reported in Southern Vietnam between January 1, 2018, and June 30, 2020. The number of infections started to increase in August 2018 (Figure 1a). Two peaks in the incidence of measles were observed in March 2019 (8.94/100,000; 95% CI: 8.64-9.25) and January 2020 (2.38/100,000; 95% CI: 2.23-2.55) (Supplementary Figure 1). The incidence (per 100,000 population) in 2018, 2019, and the first half of 2020 was 13.1 (95% CI: 12.7-13.5), 53.8 (95% CI: 53.0-54.5), and 4.8 (95% CI: 4.6-5.0), respectively. The majority of cases (61.4%) were children aged <5 years and the median age at disease onset was 3 years (range: <1-84 years). The 0-4 years age group had the highest incidence per 100,000 population, followed by the 5-14 years and 15+ years age groups. The 2019 incidence of measles was 482.9/100,000 (95% CI: 474.2-491.7) in the 0-4 years, 82.3/100,000 (95% CI: 79.9-84.7) in the 5-14 years, and 11.9/100,000 (95% CI: 11.5-12.3) in the 15+ years age groups. The resurgence heavily affected the Ho Chi Minh City, Dong Nai, and Binh Duong, accounting for 57.4% of total cases. In 2018, 5 of 20 provinces had an incidence per 100,000 population greater than the national threshold of 7.5/100,000, rising to 19 of 20 provinces in 2019 (except Lam Dong), whereas in only two provinces (Can Tho City and Hau Giang) the incidences per 100,000 population in 2020 were still higher than the national indicator (Figure 2).

Figure 1b shows the estimates of the time-dependent $R_e$ of the measles outbreak. At the early stage of the epidemic, $R_e$ was estimated at 1.46 (95% CI: 1.26-1.62). Although there was a small trough one week later, $R_e$ sharply increased and peaked to 2.34 (95% CI: 2.20-2.46) in late August 2018. The trajectory of $R_e$ was above the threshold of 1 until late January 2019 and then exhibited fluctuations between February and March 2019. $R_e$ showed a decrease below unity by the end of September 2019 before it surged again one month later with a peak of 1.16 (95% CI: 1.12-1.21). $R_e$ was close to unity for the next 2 months and then decreased further as the outbreak came to an end.

### *Spatio-temporal analysis*

The estimated parameters of the different models are summarized in Table 2. The model presented in the last column provides the best predictive performance, as it has the lowest scores of logS and RPS. The adoption of the negative binomial distribution in the model is more appropriate (estimated $\psi = 0.154$; 95% CI: 0.14-0.17) than the Poisson distribution (corresponding to $\psi \equiv 0$). In general, the model that best characterizes the measles outbreak in the Southern region is the model that incorporates vaccination coverage, includes the population effect into the spatio-temporal component, assumes spatial interaction (i.e., commuter-driven and long-range spread via the use of the power law model), and includes random effects to account for spatial heterogeneity in each of the components. The distribution of the predicted number of cases (as immersed from the selected model) captured well the observed daily cases (Supplementary Figure 2). The risk of infections was explained for 44.5% by transmission within provinces and 50.5% by transmission between provinces, whereas only 5% of the risk was attributable to the endemic component. This result

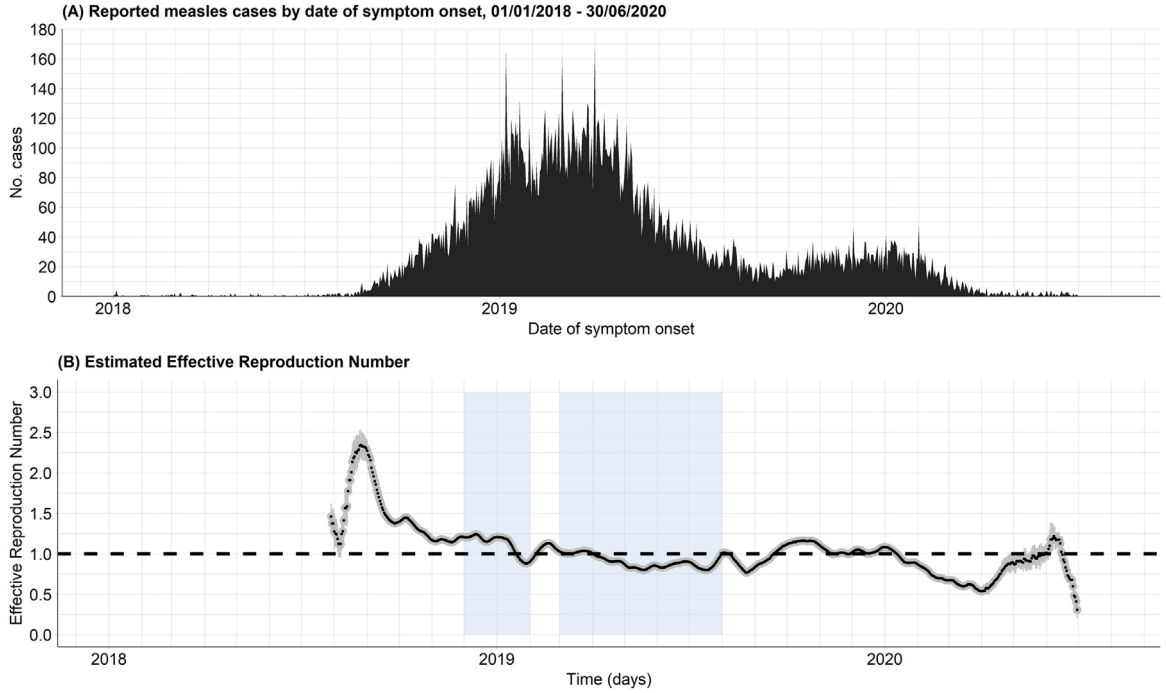


**Figure 1.** (a) Epidemic curve of measles cases by date of symptom onset in Southern Vietnam from January 1, 2018, to June 30, 2020, and (b) the corresponding effective reproduction number $R_e$ over time. The black dots show the mean estimates, and the gray zone shows 95% confidence interval. The horizontal dashed line illustrates the threshold value $R_e = 1$. The blue areas indicate the timing of supplementary immunization activities from December 2018 to January 2019 and March-July 2019.

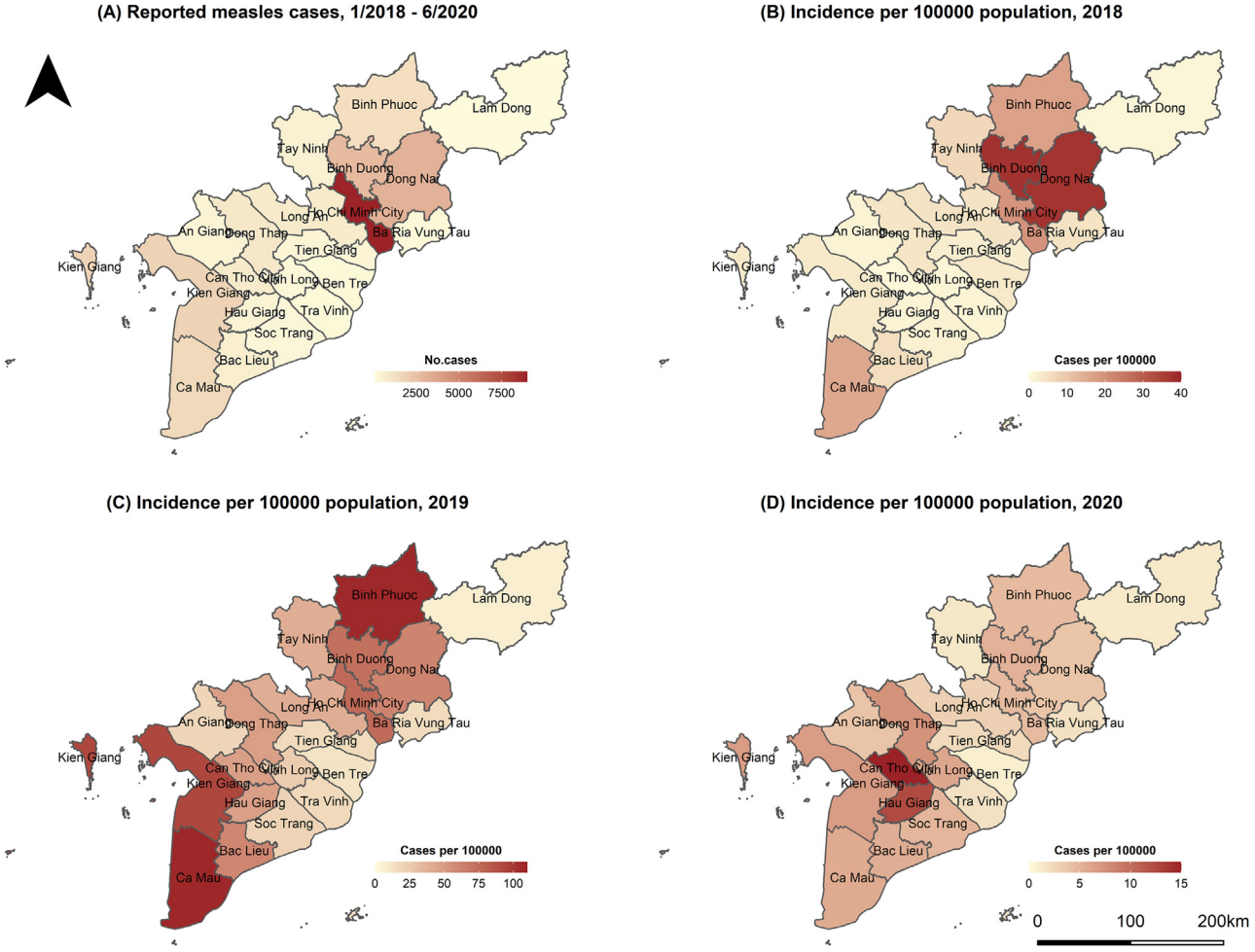


**Figure 2.** Spatial distribution of (a) the crude reported measles cases from January 1, 2018, to June 30, 2020, and (b), (c), (d) the measles incidence per 100,000 population in 2018, 2019, and the first 6 months of 2020, respectively.

**Table 2**
Parameters estimates in different models. Glossary of parameters is available in Table 1. The standard errors (SE) of the parameters are shown in parentheses.

| | | Basic Negative Binomial model | Model extension | | | |
|---|---|---|---|---|---|---|
| | | | Adding covariate (vaccination coverage) | Adding population effects | Adding the power law model | Adding random effects |
| $\ell$ | | −18,218.36 | −18,130.89 | −18,089.93 | -17,819.41 | $\ell_{pen} = -16,964.17$<br>$\ell_{marg} = -129.79$ |
| AIC | | 36,450.71 | 36,279.78 | 36,199.87 | 35,660.81 | – |
| *maxEV* | | 0.83 | 0.84 | 0.91 | 0.92 | 0.95 |
| $\psi$ | | 0.357 | 0.351 | 0.320 | 0.273 | 0.154 |
| (SE) | | (0.015) | (0.015) | (0.015) | (0.013) | (0.009) |
| Autoregressive component | $\alpha^{(\lambda)}$ (SE) | −0.511 | −0.028 | −0.118 | 0.091 | −0.105 |
| | | (0.010) | (0.064) | (0.068) | (0.070) | (0.566) |
| | $\beta_{vac}$ | – | 0.158 | 0.172 | 0.257 | 0.434 |
| | (SE) | | (0.020) | (0.022) | (0.024) | (0.167) |
| | $\sigma^2_{\lambda}$ | – | – | – | – | 0.433 |
| Spatio-temporal component | $\alpha^{(\phi)}$ (SE) | −2.997 | −3.041 | −14.710 | −18.750 | −13.060 |
| | | (0.031) | (0.032) | (0.761) | (0.594) | (4.245) |
| | $\tau$ | – | – | 0.830 | 1.223 | 0.847 |
| | (SE) | | | (0.053) | (0.041) | (0.298) |
| | $d$ | – | – | – | 1.512 | 1.848 |
| | (SE) | | | | (0.140) | (0.128) |
| | $\sigma^2_{\phi}$ | – | – | – | – | 0.489 |
| Endemic component | $\alpha^{(\nu)}$ | −17.870 | −16.760 | −16.900 | −17.230 | −18.580 |
| | (SE) | (0.091) | (0.146) | (0.151) | (0.219) | (0.322) |
| | $\alpha_{vac}$ | – | 0.320 | 0.300 | 0.403 | 0.063 |
| | (SE) | | (0.036) | (0.037) | (0.054) | (0.079) |
| | $\sigma^2_{\nu}$ | – | – | – | – | 0.076 |
| | $\beta_t$ | 0.003 | 0.003 | 0.003 | 0.003 | 0.003 |
| | (SE) | (0.0001) | (0.0001) | (0.0001) | (0.0002) | (0.0002) |
| | $A$ | 1.158 | 1.177 | 1.175 | 1.203 | 0.987 |
| | (SE) | (0.054) | (0.052) | (0.055) | (0.074) | (0.097) |
| | $\varphi$ | 2.401 | 2.410 | 2.366 | 2.418 | 2.405 |
| | (SE) | (0.018) | (0.017) | (0.018) | (0.022) | (0.030) |
| Model assessment[a] | logS ($P$-value) | 1.276 | 1.269 | 1.267 | 1.249 | 1.186 |
| | | (0.001) | (0.001) | (0.001) | (0.001) | (−) |
| | RPS | 0.780 | 0.785 | 0.759 | 0.731 | 0.660 |
| | ($P$-value) | (0.001) | (0.001) | (0.001) | (0.001) | (−) |

[a] The logarithmic score (logS) and ranked probability score (RPS) of the random effects model are compared with the remaining models. The $P$-values are calculated from the permutation test for paired observation with 999 permutations (significance level $\alpha = 0.05$).

corresponds to the estimated dominant eigenvalue of 0.95, which reflects the proportion of epidemic behavior. Substantial variation in the relative contribution of each of the three components across provinces is depicted in Figure 3 and described in Table 3. The within-locality transmission proportion varied from 4.1% in Lam Dong to 61.5% in Ho Chi Minh City (median: 23.75%). The between-locality transmission showed larger impact in most provinces with less variation in proportions, ranging from 36.1% in Ho Chi Minh City to 78.8% in Ba Ria Vung Tau (median: 67.15%). The proportion of cases attributable to the endemic component fluctuated with a median 6.7% (range: 2.4% in Ho Chi Minh City to 33.4% in Lam Dong).

The estimated effect of measles susceptibility derived from the MCV1 coverage in the autoregressive component in the selected model is clearly significant with $\beta_{vac} = 0.43$ (95% CI: 0.11-0.76). This indicates that provinces with a high susceptible proportion were associated with an increase in the number of infections in the autoregressive component. In contrast, if the number of susceptible persons in a particular province decrease (by vaccination), for example, by half, the measles incidence in the autoregressive component is estimated to decrease by 26% ($0.5^{0.43} = 0.74$; 95% CI: 0.59-0.93). However, such association was not significant in the endemic component ($\alpha_{vac} = 0.063$, 95% CI: −0.09 to 0.22). We found strong evidence of computer-driven spread when accounting for the area-specific population in the spatio-temporal component. The corresponding power of the population scaling factor $\tau = 0.85$ (95% CI: 0.26-1.43) provides such an association. In addition, the geographical spread exhibits a strong distance decay of transmission, with the decay parameter $d = 1.85$ (95% CI: 1.60-2.10). The weights $w_{r'r} = o_{r'r}^{-d}$ yield estimates of 1.00, 0.28, 0.13, 0.08, 0.05, 0.04, and 0.03 corresponding with adjacency orders 1 to 7, respectively (Supplementary Figure 3).

**Table 3**
The contribution in proportion (%) of each of the three components in the cumulative cases estimated from the selected model by province and the whole Southern region.

| Province | Estimated proportion of each component | | |
|---|---|---|---|
| | Endemic | Within-province | Between-province |
| Lam Dong | 33.4 | 4.1 | 62.5 |
| Ho Chi Minh City | 2.4 | 61.5 | 36.1 |
| Binh Phuoc | 2.8 | 34.3 | 62.9 |
| Tay Ninh | 8.4 | 25.7 | 65.9 |
| Binh Duong | 3.8 | 35.9 | 60.3 |
| Dong Nai | 3.2 | 50.7 | 46.1 |
| Ba Ria Vung Tau | 15.0 | 6.3 | 78.8 |
| Long An | 6.5 | 18.8 | 74.7 |
| Dong Thap | 6.4 | 25.2 | 68.4 |
| An Giang | 19.7 | 12.8 | 67.5 |
| Tien Giang | 17.6 | 7.1 | 75.3 |
| Vinh Long | 10.6 | 11.3 | 78.2 |
| Ben Tre | 20.4 | 12.7 | 66.8 |
| Kien Giang | 3.8 | 53.3 | 42.9 |
| Can Tho City | 6.9 | 42.1 | 50.7 |
| Hau Giang | 6.4 | 23.5 | 70.1 |
| Tra Vinh | 17.0 | 15.5 | 67.5 |
| Soc Trang | 22.2 | 10.1 | 67.7 |
| Bac Lieu | 6.3 | 24.0 | 69.7 |
| Ca Mau | 3.5 | 50.3 | 46.2 |
| Southern Vietnam | 5.0 | 44.5 | 50.5 |

The variance of random effects is largest in the autoregressive ($\sigma^2_{\lambda} = 0.433$) and spatio-temporal ($\sigma^2_{\phi} = 0.489$) components,

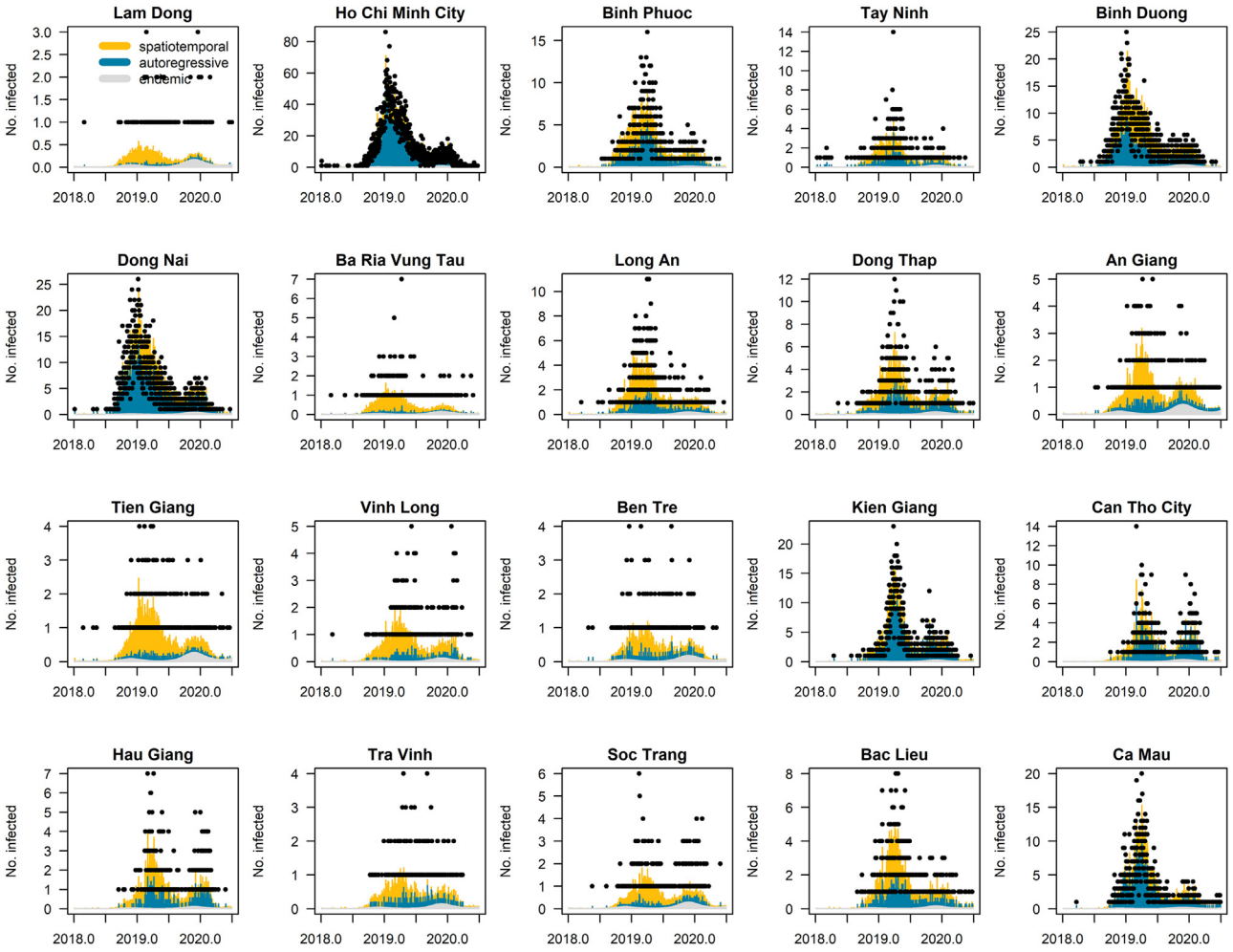


**Figure 3.** Fitted components of the random effects model for two cities and 18 provinces in Southern Vietnam between January 1, 2018, and June 30, 2020. The y-axis represents the daily number of cases and the x-axis represents the time in days. The dots indicate the observed number of daily infections. The autoregressive, the spatio-temporal, and the endemic components are illustrated by blue, orange, and gray areas, respectively.

whereas there is little variation in the random effect in the endemic component ($\sigma_v^2 = 0.076$) (Figure 4). This indicates that a substantial spatial heterogeneity of incidence levels in the epidemic component was explained by the random effects and that the heterogeneity in the endemic component was better described by the covariates in the model. The orange provinces in Figure 4a suggest that these areas have been affected by local outbreaks. Nevertheless, Binh Phuoc, Bac Lieu, Hau Giang, Dong Thap, and Binh Duong are estimated with relatively low autoregressive factors but high estimates in spatio-temporal random effects, implying that cases were more likely imported from other provinces (Figure 4b). In provinces such as An Giang, Soc Trang, Tien Giang, Ba Ria Vung Tau, and Lam Dong with the relatively high random effects in the endemic component compared with other two components, the disease dynamics exhibited more of an endemic than epidemic behavior (Figure 4c).

## Discussion

We performed a meticulous retrospective analysis of the resurgence of measles based on spatio-temporal surveillance data collected from Southern Vietnam from January 1, 2018, to June 30, 2020. The magnitude of the outbreak was illustrated by a two-peak temporal pattern, and the outbreak lasted for nearly 2 years, which was longer than any other previous outbreaks in the region (Phan Trong Lan et al., 2014; Sniadack *et al.*, 2011). Different factors could have contributed to the ending of the epidemic, such as reductions in the susceptible population caused by the epidemic itself and the implemented public health interventions (*e.g.*, supplementary immunization activities - SIAs). Though one should also note that the measures taken against the COVID-19 pandemic that started at the end of January 2020 (lockdown and social distancing, Quach *et al.*, 2021) likely further added to the interruption of measles transmission. Besides, the persistence of the outbreak was implied by the prolonged $R_e$ beyond unity during August 2018 to January 2019. Theoretically, $R_e$ reflects the impact of containment measures and the reduction of susceptible population in an epidemic (Gay, 2004; Wallinga and Teunis, 2004). $R_e$ below one was in accordance with the timing of SIAs (targeted children aged 1-5 years) between March and July 2019, illustrating that these SIAs may have contributed in reducing the susceptible population and thus mitigating the epidemic. However, its applicability to assess the effectiveness of SIAs may be limited in our study because of two possible reasons. First, the calculation relied on the aggregated observed cases of all provinces instead of province-specific estimates. Second, only 67% of the districts of 18 provinces in the South (except Ba Ria Vung Tau and An Giang) were involved in the national SIAs. Moreover, interventions other than the vaccination strategy could have contributed to the change of $R_e$ but are not explicitly discussed here because of lack of information. To as-

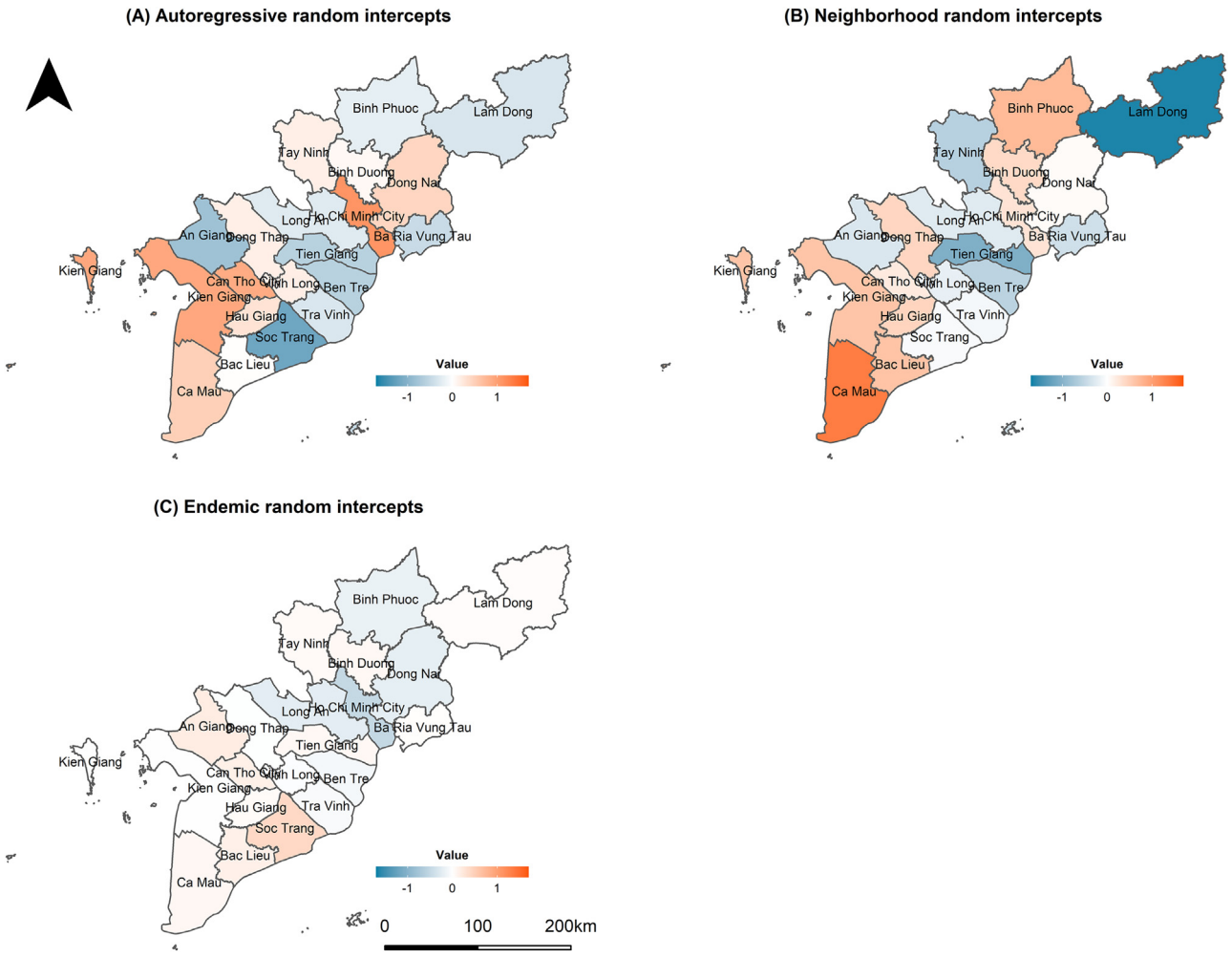


**Figure 4.** The estimated province-specific random intercepts in the random effects model. The random intercepts $b_r^{(\lambda)}$, $b_r^{(\phi)}$, $b_r^{(\nu)}$ of the autoregressive, spatio-temporal, and endemic components, respectively, are visualized in maps.

sess the impact of control measures on measles incidence, there is a need to have in-depth surveys or reviews of data such as vaccination status of individuals, reported administrative MCV coverage from routine programs, and time frame of implemented measures with geographical extent, targeted groups and size, etc., in combination with measles surveillance data. Based on case numbers and knowledge of the serial interval, our estimated $R_e$ should be considered a realized $R_e$ that differs from the expected $R_e$, which can be calculated based on the population immunity levels and other remediable factors (*e.g.*, context-specific contact patterns, population size). Whereas the latter is to determine the disease resurgence risk (Béraud *et al.*, 2018; Funk *et al.*, 2019; Hens *et al.*, 2015), the former allows us to retrospectively observe the actual evolution during the epidemic. We believe that both measures offer benefits in an epidemic.

To study the spatio-temporal spread of the disease, stochastic models such as compartmental models (Lau *et al.*, 2020; Xia *et al.*, 2004; Yang, 2020) and chain-binomial models (Robert *et al.*, 2020) are desirable. These models describe the infection process at the individual level. However, they require information on susceptibility that is not always available in surveillance data and sometimes require intensive calculations. In contrast, the endemic-epidemic approach allows us to use the routinely collected surveillance data and flexibly incorporate potential variables that may have a significant impact on the spatio-temporal spread of the disease. In addition, the model parameters are easily estimated using regular optimization techniques (*e.g.*, maximum likelihood) (Held *et al.*, 2005; Paul *et al.*, 2008). An important feature of our modeling strategy is that it distinguishes between cases transmitted within or between regions, taking into account endemic behavior. This is useful in determining appropriate public health interventions for specific areas. For instance, implementation of more stringent measures is necessary for provinces with high local transmission, whereas enhancing routine surveillance is more appropriate for “endemic-transmission” provinces.

The modeling results revealed that heterogeneity in vaccination coverage between geographical units has a strong link to measles incidence. It is anticipated that the local vaccination coverage has been shown to be useful in speculating about at-risk regions. Provinces with lower vaccination coverage were associated with increasing cases in the localities. In our context, Binh Phuoc, for example, had the lowest 2019 MCV1 coverage in the region and was one of the worst affected provinces in that year. Our study also showed that local coverage of the first dose of measles vaccine is a good indicator of the level of immunity in the population, consistent with the findings of Robert *et al.* (2022). Nevertheless, immunity levels depend on age groups (Béraud *et al.*, 2018; Funk *et al.*, 2019; Hens *et al.*, 2015) and outbreaks will occur if there are immunity gaps in the age cohorts. The predominance of children aged under 5 years (61.4% of total cases) in the study could be due to the low vaccination coverage among them. In the 2013-2014 outbreak, a cross-sectional study demonstrated that only 54.9% of

children aged 9 months-10 years completed the two-dose schedule in contrast with the 82.4% vaccination coverage reported in Ho Chi Minh City in the same year (Cuong *et al.*, 2019). Moreover, a serosurvey in Northern Vietnam in 2013-2014 also revealed that 40% to 80% of children aged <5 years were seropositive (Choisy *et al.*, 2019). Such level of protection is obviously inadequate to prevent measles infections in this age group. In addition, 17.3% of cases aged <9 months in our study were found to be infected before they were eligible for routine vaccination. This is likely due to a strong decay of maternal antibodies of measles in infants from immune mothers, making them susceptible at an early stage in life (Guerra *et al.*, 2018; Leuridan *et al.*, 2010). A small fraction of young adult cases in the study were not protected by vaccination in the past, especially during the period when measles vaccination coverage was scaling up to the routine immunization program (1983-1989) (Sniadack *et al.*, 2011). Our study re-emphasizes that vaccination has largely contributed to the significant reduction in measles incidence. To better understand the relative contribution of under-vaccination to further disease occurrence, it is beneficial and necessary to critically evaluate measles vaccine uptake in the population by both age and space. Serological surveys can provide useful information in this regard.

Spatial patterns in our outbreak, as expected, were shared by two major drivers including commuter movement and long-range transmission. Specifically, 36.1% to 78.8% of cases in 20 provinces were introduced by human mobility outside their home residence. Adding a population effect in the spatio-temporal component successfully reflected the idea that a denser population increases the risk of importing cases from neighbors. Ho Chi Minh City, Dong Nai, and Binh Duong are the most populous provinces in the South, and hence, a larger number of infections were prone to importation from neighboring areas to such metropoles. In the absence of movement data, our analysis also highlighted the substantial impact of population traveling from different levels of neighboring orders on the disease dissemination. This is comparable with the transmission pattern in Cameroon and China (Parpia *et al.*, 2020; Qin *et al.*, 2019). The behavior of rural-to-urban and urban-to-rural short-term movement could worsen the risk of outbreaks in different localities. Many clusters and small outbreaks were discovered in shelters located within industrial zones, with a floating population, especially in metropolitan provinces. Such sub-population is usually seen with low immunization coverage because of socioeconomic inequalities, which are barriers to EPI (Cuong *et al.*, 2019; Kien *et al.*, 2017; Nguyen *et al.*, 2019). In addition, the Lunar New Year (between late January and February), which is marked by high human mobility in weeks before and after the holiday, was an important contributor to measles diffusion (Sniadack *et al.*, 2011; Yang *et al.*, 2017). The efflux of infected individuals from urban cities into distant provinces might have introduced the disease in rural communities. This mechanism was consistent with the occurrence of the first epidemic peak in March 2019. Caution about the potentiality of increased incidence of measles facilitated by between-locality transmission, especially during holidays, should be concerted in future control strategies, *e.g.*, in health promotion and vaccination programs in under-immunized areas.

In our model, a substantial level of difference in reporting was captured by using random effects. Underreporting is common in any surveillance system. In our setting, measles cases could have been misreported due to diagnosis practices (*e.g.*, diagnosed as typhus fever [ICD10 A75] instead of measles [ICD10 B05]) and lack of medical attention in older patients or community cases. Specifically, children are prone to hospitalization more frequently than adults and might be diagnosed with measles because of classic symptoms, whereas older cases may be less likely to be suspected for measles owing to milder illness with less intense symptoms (Augusto *et al.*, 2018; Barrett *et al.*, 2018). Moreover, potential sources of infections can possibly import from areas outside the study setting including cross-border infections (i.e., edge effects). Future research should focus on the impact of underreporting during the measles epidemic and expanding the spatio-temporal analysis at regional and national levels.

We recorded several limitations. First, we assumed a homogeneous mixing population without accounting for social contact patterns, which at least partly are available for Vietnam (Horby *et al.*, 2011) and which may provide a better understanding of the transmission within and between age and/or gender groups (Meyer and Held, 2017). Second, the susceptible population might be overestimated because we only used MCV1 coverage as a proxy to infer susceptibility to measles in the model, regardless of age. Given that the immunity levels are age-dependent (Béraud *et al.*, 2018; Funk *et al.*, 2019; Hens *et al.*, 2015), an age-stratified analysis would be recommended, provided that data on age-specific MCV1 coverage would be available. Third, the calculation of the reproduction numbers may have potential bias due to the assumption of serial interval, incomplete case observation (*e.g.*, underreporting), and the choice of time window (Cori *et al.*, 2013; Gostic *et al.*, 2020). Finally, we did not assume (spatially) correlated random effects, which might be more satisfactory to account for the unobserved heterogeneities because, for example, effects are presumably more alike in adjacent areas than in distant areas (Paul and Held, 2011). However, the limited overdispersion in our final model indicates that the model performed reasonably well.

In conclusion, our study highlights that the measles transmission across provinces was characterized by the heterogeneous contribution of the endemic and observation-driven epidemic components, which was influenced by factors such as vaccination coverage and spatial interaction between localities, especially nearby provinces. The estimates $R_e(t)$ helped explain the prolonged duration of the measles epidemic. Strengthening surveillance systems is recommended and further research is essential to understand the relative contribution of the population immunity and control measures in the measles epidemic.

## Author contributions

T.H.T.N participated in data acquisition, analysis, and interpretation of data, and writing the original draft. T.V.N, Q.C.L, and T.V.H helped in interpretation of the results and reviewed the manuscript. C.F and N.H were involved in study conception, design and analysis, interpretation of the results and supervision, and critical revision of the manuscript. All authors approved the final version of the manuscript.

## Ethical approval statement

This study is a model study using data on reported measles cases from the public health surveillance system in Vietnam. The data provided for analysis of this study did not contain patients' identification. Therefore, this study did not require ethical approval.

## Funding

This research did not receive any specific grant from funding agencies in the public, commercial, or not-for-profit sectors.

## Declaration of Competing Interest

The authors have no competing interests to declare.

## Acknowledgments

We would like to thank the VLIR-UOS for awarding T.H.T.N. a scholarship to study the Master of Epidemiology at the University of Antwerp, Belgium. We are pleased to acknowledge the Pasteur Institute in Ho Chi Minh City including the Board of Directors for supporting the research endeavor in terms of data use, colleagues of the Outbreak Control Unit (Pham Duy Quang, Nguyen Thi Phuong Thuy, Tran Cong Kha, Doan Ngoc Minh Quan, Nguyen Quoc Kien, Tran Anh Tuan, Phan Thi Ngoc Uyen, Nguyen Viet Thinh, Hoang Thi Lien, and Phan Cong Hung), and the EPI Unit (Hoang Anh Thang, Chau Van Luom, Truong Cong Hieu, Vo Ngoc Quang, Nguyen Dieu Thuy, Nguyen Thi Huyen, Phan Thi Quynh Tram, Vien Dang Khanh Linh, Nguyen Thi Thu Trang, Nguyen Van Hoang, Tran Quang Trung, Trinh Trung Truc, Tran Thanh Hai) for their huge efforts and enthusiasm in case monitoring, surveillance and contact tracing, outbreak investigation, and launching the supplementary immunization activities during the measles outbreak. We would also like to acknowledge the large contribution of 20 Provincial Centers for Disease Control and Prevention in two cities and 18 provinces in Southern Vietnam in the EPI National Project.

## Supplementary materials

Supplementary material associated with this article can be found, in the online version, at doi:10.1016/j.ijid.2022.07.055.

## References

Andrianou XD, Del Manso M, Bella A, Vescio MF, Baggieri M, Rota MC, et al. Spatiotemporal distribution and determinants of measles incidence during a large outbreak, Italy, September 2016 to July 2018. Euro Surveill 2019;24.

Augusto GF, Cruz D, Silva A, Pereira N, Aguiar B, Leça A, et al. Challenging measles case definition: three measles outbreaks in three Health Regions of Portugal, February to April 2018. Euro Surveill 2018;23.

Barrett P, Cotter S, Ryan F, Connell J, Cronin A, Ward M, Fitzgerald R, Lynch C, Margiotta T. Outbreak Control Team. A national measles outbreak in Ireland linked to a single imported case, April to September, 2016. Euro Surveill 2018;23.

Béraud G, Abrams S, Beutels P, Dervaux B, Hens N. Resurgence risk for measles, mumps and rubella in France in 2018 and 2020. Euro Surveill 2018;23.

Choisy M, Trinh ST, Nguyen TND, Nguyen TH, Mai QL, Pham QT, et al. Sero-prevalence surveillance to predict vaccine-preventable disease outbreaks; a lesson from the 2014 measles epidemic in Northern Vietnam. Open Forum Infect Dis 2019;6 ofz030.

Cori A, Ferguson NM, Fraser C, Cauchemez S. A new framework and software to estimate time-varying reproduction numbers during epidemics. Am J Epidemiol 2013;178:1505–12.

Cuong HQ, Nguyen HX, Van Hau P, Ha NLK, Lan PT, Mounts A, et al. Gap in measles vaccination coverage among children aged 9 months to 10 years in Ho Chi Minh City, Viet Nam, 2014. West Pac Surveill Resp J 2019;10:39–45.

Czado C, Gneiting T, Held L. Predictive model assessment for Count Data. Biometrics 2009;65:1254–61.

Funk S, Knapp JK, Lebo E, Reef SE, Dabbagh AJ, Kretsinger K, Jit M, Edmunds WJ, Strebel PM. Combining serological and contact data to derive target immunity levels for achieving and maintaining measles elimination. BMC Med 2019;17:180.

Gay NJ. The theory of measles elimination: implications for the design of elimination strategies. J Infect Dis 2004;189:S27–35.

General Statistics Office of Vietnam. The completed results of the 2019 Vietnam population and housing census. http://tongdieutradanso.vn/12-completed-results-of-the-2019-census.html, 2020 (accessed 29 January 2021 ).

Gostic KM, McGough L, Baskerville EB, Abbott S, Joshi K, Tedijanto C, et al. Practical considerations for measuring the effective reproductive number, Rt. PLoS Comput Biol 2020;16.

Guerra FM, Crowcroft NS, Friedman L, Deeks SL, Halperin SA, Severini A, et al. Waning of measles maternal antibody in infants in measles elimination settings - a systematic literature review. Vaccine 2018;36:1248–55.

Held L, Höhle M, Hofmann M. A statistical framework for the analysis of multivariate infectious disease surveillance counts. Stat Modell 2005;5:187–99.

Held L, Paul M. Modeling seasonality in space-time infectious disease surveillance data. Biom J 2012;54:824–43.

Hens N, Abrams S, Santermans E, Theeten H, Goeyvaerts N, Lernout T, Leuridan E, et al. Assessing the risk of measles resurgence in a highly vaccinated population: Belgium anno 2013. Euro Surveill 2015;20:20998.

Herzog SA, Paul M, Held L. Heterogeneity in vaccination coverage explains the size and occurrence of measles epidemics in German surveillance data. Epidemiol Infect 2011;139:505–15.

Horby P, Pham QT, Hens N, Nguyen TTY, Le QM, Dang DT, et al. Social contact patterns in Vietnam and implications for the control of infectious diseases. PLOS ONE 2011;6:e16965.

Kien VD, Van Minh H, Giang KB, Mai VQ, Tuan NT, Quam MB. Trends in childhood measles vaccination highlight socioeconomic inequalities in Vietnam. Int J Public Health 2017;62:41–9.

Lau MSY, Becker AD, Korevaar HM, Caudron Q, Shaw DJ, Metcalf CJE, et al. A competing-risks model explains hierarchical spatial coupling of measles epidemics en route to national elimination. Nat Ecol Evol 2020;4:934–9.

Leuridan E, Hens N, Hutse V, Ieven M, Aerts M, Van Damme P. Early waning of maternal measles antibodies in era of measles elimination: longitudinal study. BMJ 2010;340:c1626.

Meyer S, Held L. Power-law models for infectious disease spread. Ann Appl Stat 2014;8:1612–39.

Meyer S, Held L. Incorporating social contact data in spatio-temporal models for infectious disease spread. Biostatistics 2017;18:338–51.

Meyer S, Held L, Höhle M. Spatio-Temporal Analysis of Epidemic Phenomena Using the R package surveillance. J Stat Softw 2017;77:2017.

Nguyen CTT, Grappasonni I, Scuri S, Nguyen BT, Nguyen TTT, Petrelli F. Immunization in Vietnam. Ann Ig 2019;31:291–305.

Nimpa MM, Andrianirinarison JC, Sodjinou VD, Douba A, Masembe YV, Randriatsarafara F, et al. Measles outbreak in 2018–2019, Madagascar: epidemiology and public health implications. Pan Afr Med J 2020;35:84.

Parpia AS, Skrip LA, Nsoesie EO, Ngwa MC, Abah Abah AS, Galvani AP, et al. Spatio-temporal dynamics of measles outbreaks in Cameroon. Ann Epidemiol 2020;42 64–72.e3.

Patel MK, Goodson JL, Alexander JP, Kretsinger K, Sodha SV, Steulet C, Gacic–Dobo M, Rota PA, McFarland J, Menning L, Mulders MN, Crowcroft NS. Progress toward regional measles elimination — worldwide, 2000–2019. MMWR Morb Mortal Wkly Rep 2020;69:1700–5.

Paul M, Held L. Predictive assessment of a non-linear random effects model for multivariate time series of infectious disease counts. Stat Med 2011;30:1118–36.

Paul M, Held L, Toschke AM. Multivariate modelling of infectious disease surveillance data. Stat Med 2008;27:6250–67.

Phan Trong Lan, Nguyen Vu Thuong, Ho Vinh Thang, Phan Cong Hung, Vo Ngoc Quang, Nguyen Thi Phuong Lan, et al. Epidemiological characteristics of measles outbreak in Southern region Vietnam, 2013 - 2014 [in Vietnamese]. Vietnam Journal of Preventive Medicine 2014;3(152):19.

Pogka V, Horefti E, Evangelidou M, Kostaki EG, Paraskevis D, Flountzi A, et al. Spatio-temporal distribution and genetic characterization of measles strains circulating in Greece during the 2017–2018 outbreak. Viruses 2020;12:1166.

Qin S, Ding Y, Yan R, He H. Measles in Zhejiang, China, 2004–2017: population density and proportion of floating populations effects on measles epidemic. Health Secur 2019;17:193–9.

Quach HL, Nguyen KC, Hoang NA, Pham TQ, Tran DN, Le MTQ, et al. Association of public health interventions and COVID-19 incidence in Vietnam, January to December 2020. Int J Infect Dis 2021;110:S28–43.

Robert A, Kucharski AJ, Funk S. The impact of local vaccine coverage and recent incidence on measles transmission in France between 2009 and 2018. BMC Med 2022;20:77.

Robert A, Kucharski AJ, Gastañaduy PA, Paul P, Funk S. Probabilistic reconstruction of measles transmission clusters from routinely collected surveillance data. J R Soc Interface 2020;17.

Sniadack DH, Mendoza-Aldana J, Huyen DT, Van TT, Cuong NV, Olive JM, et al. Epidemiology of a measles epidemic in Vietnam 2008–2010. J Infect Dis 2011;204:S476–82.

Vietnam Ministry of Health. Decision No.4845/QD-BYT dated, 05/12/2012 on Guidance for Measles and Rubella Surveillance and Monitoring [in Vietnamese]. http://tiemchungmorong.vn/vi/content/quyet-dinh-ban-hanh-huong-dan-giam-sat-va-phong-chong-benh-soi-rubella.html, 2012 (accessed 02 February 2021).

Vietnam Ministry of Health. Desicion No.137/QD-BYT dated 17 January 2020 regarding to Planning for Prevention of Infectious Diseases in 2020 [in Vietnamese].

Vink MA, Bootsma MCJ, Wallinga J. Serial intervals of respiratory infectious diseases: a systematic review and analysis. Am J Epidemiol 2014;180:865–75.

Wallinga J, Teunis P. Different epidemic curves for severe acute respiratory syndrome reveal similar impacts of control measures. Am J Epidemiol 2004;160:509–16.

Xia Y, Bjørnstad ON, Grenfell BT. Measles metapopulation dynamics: a gravity model for epidemiological coupling and dynamics. Am Nat 2004;164:267–81.

Yang W. Transmission dynamics of and insights from the 2018–2019 measles outbreak in New York City: a modeling study. Sci Adv 2020;6:eaaz4037.

Yang W, Wen L, Li SL, Chen K, Zhang WY, Shaman J. Geospatial characteristics of measles transmission in China during 2005–2014. PLoS Comput Biol 2017;13.

Zucker JR, Rosen JB, Iwamoto M, Arciuolo RJ, Langdon-Embry M, Vora NM, et al. Consequences of under vaccination - measles outbreak, New York City, 2018–2019. N Engl J Med 2020;382:1009–17.